JOURNAL OF MATERIALS SCIENCE **36** (2001) 1001–1006

# High sinterability of Ca-PZT, synthesized by polymeric and partial oxalate process

R. S. NASAR, M. CERQUEIRA
*Departamento de Quimica, UFRN, Natal/R.N., 59078-970 Caixa Postal 1662, Brasil*
N. DUBOC, E. LONGO
*Departamento de Quimica, UFSCar, São Carlos/S.P., 13565-905, Brasil*
J. A. VARELA
*Instituto de Quimica, UNESP, Araraquara/S.P., 14800-900, Brasil*

This study includes Ca-PZT in the morphotropic phase boundary, MPB process combining the Pechini method, (ZT) and the Partial oxalate method (Ca-PZT) by obtaining single phase particles of ZT phase with a high specific surface area (~110 $m^2/g$ at 550° C) and narrow particle size distribution. Lead and calcium oxalates were precipitated onto the ZT particle surface and reacted to a solid state interface ZT/Ca-PZT/PbO-CaO. A deviation of a coexistence region from $F_T$- and $F_R$-phases to $F_R$-phase (Zr rich region) was observed. Strong surface area reduction occurs by Ca-PZT crystallization at about 700°C, and demonstrated high sinterability (2.40 $m^2/g$ – 350 nm) with apparent densities near to 99.9%. Different processing methods did not demonstrate superior results. Studies of calcined powder shows a high sinterability of powder calcined 3 h at 700° C and sintered 3 h at 1000°C coming up to 99.8% of relative density.

## 1. Introduction

PZT ceramics as ferroelectric and piezoelectric materials have excellent scientific interest and a variety of technological applications [1, 2]. Additions of metals and rare earths [3] in $ABO_3$ perovskite structure lead to an optimization effect of its properties. However, factors such as synthesis, method of powder formation [4], calcination and sintering [5] increase the apparent density with a consequent improvement of its properties. Among various PZT compositions Zr/Ti (0.53/0.47) has excellent electrical properties. According to some authors [6, 7] compositions of Zr/Ti ratio between $0.52 \leq x \leq 0.54$ in the morphotropic phase boundary region (MPB) could have tetragonal phase ($F_T$) (Ti rich region), rhombohedral phase ($F_R$) (Zr rich region), however a coexistence of $F_T$ and $F_R$ phase could occur [8, 9]. At temperatures higher than the Curie temperature it shows paraelectric cubic phase, ($P_C$).

Traditional oxide mixtures could lead to intermediate reactions such as lead titanate, (PT) and lead zirconate, (PZ) phase formation [10]. A consequent agglomerated powder with poor homogeneity and variable composition (compositional fluctuation) caused electric property degradation.

Various chemical synthesis methods as sol-gel [11], precipitation [5], organic precursor synthesis [12], have been used due to formation of fine powder with stoichiometric control and without cations segregation after calcination that leads to high densities after sintering. Fernandes *et al.* [13] used sol-gel method with EDTA agent and obtained PZT powder at 450° C. The same method was used by Muralidharam *et al.* [14] who obtained nanometer particles of PZT at temperatures about 600° C.

Synthesis of PZT using cores [15] of $F_T$ and $F_R$ phases and alcohoxides as precursors shows densities about 7870 $kg/m^3$, 2 h at 1000°C, and surface area of 8.9 $m^2/g$. Kim *et al.* [16], obtained reactive powder PZT, with high density after sintering by solid state reaction below of 1000° C. Partial chemical methods used by Kakegawa *et al.* [6] and Yamamoto [4] decreased the compositional fluctuation and formed a highly reactive powder. Yamamoto synthesized ZT = (zirconium titanate) by hydrothermal method and precipitated $PbC_2O_4$ onto the crystalline surface of ZT particles obtaining PZT by solid state reaction. The powder characteristics and the sintering process lead to a homogeneous microstructure and high density.

Kimura *et al.* [17] synthesized $ZrTiO_4$ by precipitation at 750°C, reacted with PbO particles, obtaining PZT. Citrate solutions of Zr, Ti and Pb of different compositions were calcined obtaining $F_T$ PZT phase at 700°C and $F_R$ phase at 800°C. Choy *et al.* [18] obtained a stoichiometric fine powder at 500°C by using a co-precipitation method. Precipitated powder of PZT by Rao *et al.* [19] was sintered and showed high density at 900°C.

Cerqueira *et al.* [12] synthesized ZT by the Pechini method and partial oxalate [20]. Surface area of about 40 $m^2/g$ with high homogeneity and sinterability lead to dense PZT.

TABLE I Precursors used for synthesis of Ca-PZT

| Reagents | Origin | Purity |
|---|---|---|
| IV Titanium propoxide | Aldrich | 99.9 |
| IV Zirconium propoxide | Aldrich | 99.9 |
| Lead nitride | E. Merk | 99.9 |
| Calcium nitride | Riedel-deHaen | 99.7 |
| Oxalic acid | E. Merk | 99.9 |

Some works [21, 22] demonstrated that additions of metals of periodic Table II A, such as Mg, Ca, Sr and Ba to PZT did not lead to densities near to theoretical. Thus, the subject of the present work is a synthesis of $(Zr_{0.53}Ti_{0.47})O_2$ phase by Pechini method, a final synthesis by partial oxalate method and a study of powder sinterability of $Pb_{0.99}Ca_{0.01}(Zr_{0.53}Ti_{0.47})O_3$.

## 2. Experimental procedure

Table I shows analytical grade reagents for the chemical synthesis of Ca-PZT. Two stages of synthesis were carried out, such as titanium zirconate phase, (ZT) by the Pechini method and Pb with calcium oxides onto ZT particles, Ca-PZT by partial oxalate method.

### 2.1. Synthesis by the Pechini method

Zirconium and titanium citrates were prepared by using zirconium (-IV) propoxide and titanium (-IV) isopropoxide respectively with citric acid at 90°C. Zirconium and titanium citrates were mixed separately in ethylene glycol at 90°C. A sterification reaction between 90°C and 120°C for 30 min. was used. A polymerization process at 120°C and decomposition at 320° C/2 h lead to a dark powder formation. The powder was grounded, sieved at 200 mesh and calcined for 3 h between 550° C and 700° C, giving monophasic $ZrTiO_4$. A cation mixture of Zr/Ti with a molar ratio of 0.53/0.47 was prepared.

### 2.2. Ca-PZT synthesis by partial oxalate method

ZT crystalline powder was dispersed in water media and oxalic acid was added to the solution. Lead and calcium nitrate solutions with stoichiometric molar ratio of 0.99/0.01 respectively were dripped into the solution and simultaneously precipitated onto the ZT surface at $pH = 12$ using ammonium hydroxide. The precipitated mass of $ZT/(PbC_2O_4\text{-}CaC_2O_4)$ was filtered, water washed and heated 12 h at 100°C/12 h. The dried powder was calcined 3 h between 600° C and 800° C using a heating rate of 10°C/min, then granulated and sieved at 325 mesh and the phases were analyzed by XRD method.

### 2.3. Characterization

Both, ZT and Ca-PZT phases were analyzed by X-Ray diffraction pattern using a Siemens diffractometer model D-5000, with $K\alpha Cu$ radiation and carbon monochromator. Decomposition of lead and calcium oxalates were observed by thermal analysis (DTA) and thermogravimetric analysis (TG) from ambient temperature up to 1000°C. Surface area and distribution of average particle size were obtained by an ASAP 2000 model, micromeretics and a sedigraph 2000, micromeretics, respectively. Qualitative analysis of powder by the Rietveld method [23] shows the presence of different ferroelectric phases at different temperatures.

### 2.4. Crystal size

Peaks of (111) planes of Ca-PZT, determined the crystal size by using the Sherrer equation:

$$D = \frac{\lambda K}{(\beta \cos\theta)} \tag{1}$$

where, $D$ is the crystal size, $\lambda$ is the wavelength $(Cu\,K_{\alpha_1})$, $K$ a constant and $\beta$ is the half-width of diffracted peak. As a correction for instrumental line broadering

$$\beta = \sqrt{B^2 - b^2} \tag{2}$$

was applied, where, $B$ is the half-width of the Ca-PZT $(111)_R$ peak and $b$ is the half-width of (004) plane of metallic silicon as an internal pattern. Only one plane analysis will not be sufficient for a final conclusion, considering that different shapes and sizes of crystals could occur. In this study, the diffraction peak profile was fitted using a pseudo-Voigt function to calculate the full width at half maximum (FWHM).

## 3. Results and discussion

Fig. 1 shows an analysis of the X-Ray diffraction pattern from the amorphous resin until the ZT crystalline single phase formation at about 700° C. Final decomposition of resin with an increase of crystallinity was observed higher than 550° C. Similar results were obtained by Navio *et al.* [24] that who reported the synthesis of ZT at 650°C by using the co-precipitation method. The use of polymeric precursors in ZT synthesis by Leite *et al.* [25] shows 80% of ZT phase formation at 550° C. ZT phase obtained by polymeric precursor method

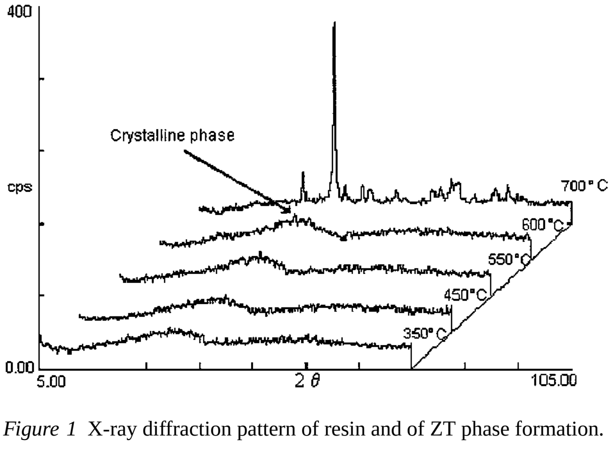

*Figure 1* X-ray diffraction pattern of resin and of ZT phase formation.

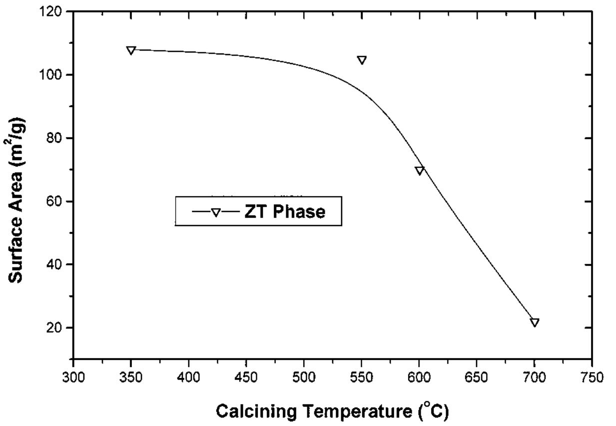

*Figure 2* Surface area of calcined powder of ZT phase from 350° C to 700° C/3 h.

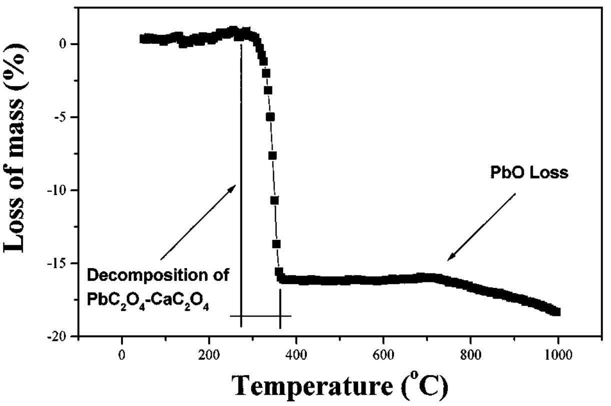

*Figure 3* Thermogravimetric analysis, TG of ZT/$PbC_2O_4$-$CaC_2O_4$ decomposition.

[12] was analyzed by FT-IR and XRD and showed high reproducibility of phase and powder characteristics. A solid state reaction between $TiO_2$ and $ZrO_2$ required high temperatures (>1000°C) to form a single ZT phase, and intermediate phases could occur. Fig. 2 shows the surface area of about 110 m$^2$/g at 350°C decreasing to 22 m$^2$/g at 700°C. The high decreases of surface area at approximately 550°C is coincident with the formation of ZT crystalline phase. Kimura *et al.* [17] processed ZT by using the co-precipitation method and obtained minor values of surface area and temperature for phase formation.

Fig. 3 shows a thermogravimetric analysis, TGA of ZT/$PbC_2O_4$-$CaC_2O_4$ mixture. Between 250°C and 380°C a decomposition of oxalates onto the particles of ZT phase was observed. Analysis by XRD (Fig. 1.) did not show crystallinity of powder lower than 600°C during the calcination. Peaks of PbO (100%) phase indicated formation of a crystalline interface between the ZT and PbO-CaO phases. Formation of Ca-PZT phase at approximately 700°C, observed by XRD was coincident with a loss of mass by TGA. The DTA curve, Fig. 4 shows an oxalate decomposition by an endothermic reaction. The peaks that are shown by XRD (≈600°C) of PbO and Ca-PZT phases crystallization did not appear clearly by DTA analysis. The Ca-PZT phase growth across a PbO-CaO/Ca-PZT/ZT interface at the sense of the external surface of the particle with a complete reaction near to 700 °C and was not detected by DTA.

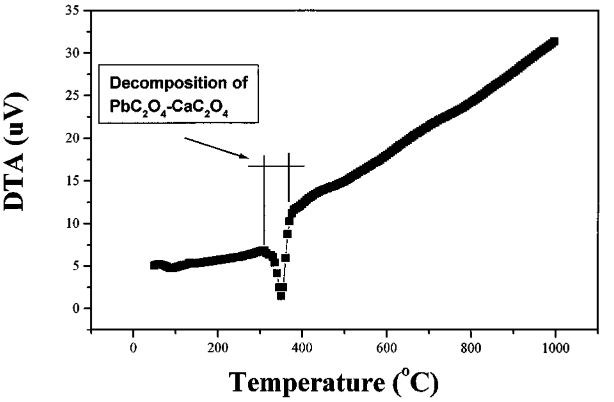

*Figure 4* Differential thermal analysis, DTA of ZT/$PbC_2O_4$-$CaC_2O_4$ decomposition.

Fig. 5 shows the analysis by X-ray diffraction pattern of calcined powder at 400°C demonstrating peaks of PbO phase and Ca-PZT phase formation at about 700°C, they are not clearly observed by TG-DTA. Due to small concentrations of calcium in PZT no peaks of this phase were observed by XRD. Two simultaneous reactions for the Ca-PZT formation occur, such as:

$$\mathrm{ZT} + \mathrm{PbC_2O_4} \rightarrow \mathrm{PbO} + \mathrm{CO} + \mathrm{CO_2}, \tag{3}$$

$$\mathrm{ZT} + \mathrm{CaC_2O_4} \rightarrow \mathrm{CaO} + \mathrm{CO} + \mathrm{CO_2}, \tag{4}$$

$$\mathrm{ZT} + \mathrm{PbO} + \mathrm{CaO} \rightarrow \mathrm{Ca} - \mathrm{PZT}. \tag{5}$$

Close to the contact regions of ZT particles and PbO-CaO phases an interface formation of Ca-PZT crystalline phase occurs with growth between 550° and 800°C. From 700°C to 750°C a coexistence between $F_T$ (Ferroelectric tetragonal phase) and $F_R$ (ferroelectric rhombohedral phase), was observed Fig. 6a. Investigations about the MPB show the same results [14,15]. However, higher than 750°C a dislocation happens from $F_T$ and $F_R$ (Ti rich region) to $F_R$ (Zr rich region in the phase's diagram), Fig. 6b occurs. These results are according to Cerqueira *et al.* [26] that obtained $F_R$ phase processing Ca-PZT (0.53/0.47) in MPB by co-precipitation method. According to certain authors [6–8] a Zr and Ti migration into the lattice happens due to a likely difference of chemical potential caused by non-homogeneous microregions. Such experimental evidences demonstrated that a strong coordination between atoms of Ca and Ti forms a stable $CaTiO_3$ favouring the growth of $F_R$ phase in Ca-PZT.

Fig. 7 shows the surface area of a mixture of ZT/PbO-CaO and Ca-PZT phases mixture demonstrating a decrease from 3.25 m$^2$/g at 600°C to 1.20 m$^2$/g at 800°C for the Ca-PZT phase. The Ca-PZT phase was formed and new particles were incorporated, which showed a strong surface area reduction as a function of the temperature. The kinetics of particle growth has been optimized for temperatures of calcination close to 600° C because at this temperature all organic material is decomposed and the phases show high crystallinity which avoids interference with mass-transport process. During the calcination two diffusion processes occur: At first a diffusion process of $Pb^{+2}$ and $Ca^{+2}$ into the PZT lattice (by interface); second by an agglomeration

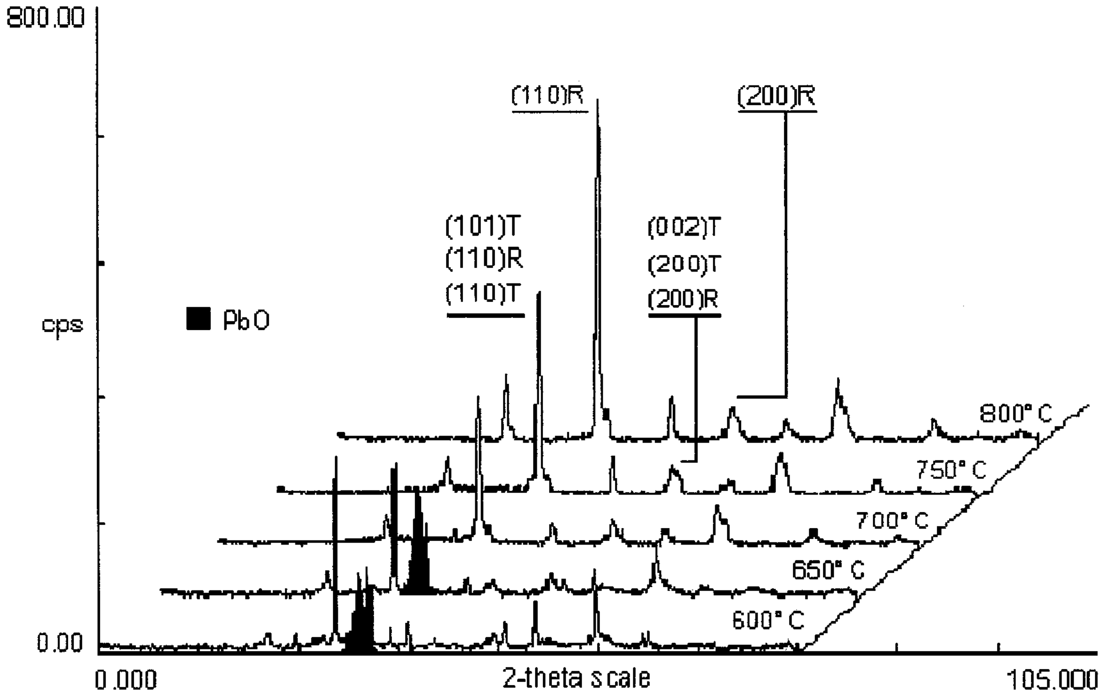

*Figure 5* X-ray diffraction pattern of Ca-PZT formation from 600° C to 800° C/3 h.

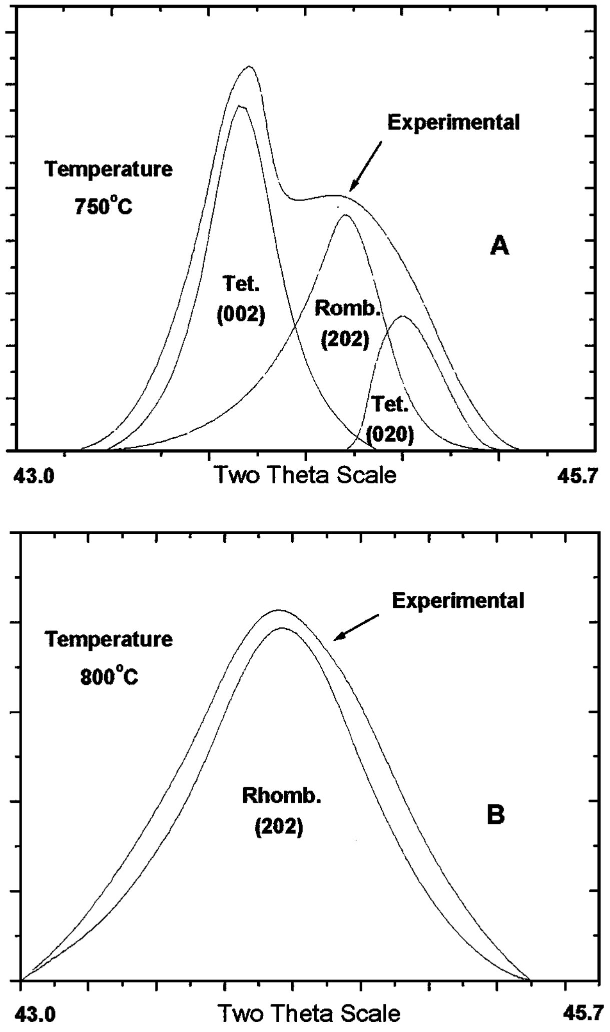

*Figure 6* Fit and deconvolution by Lorentzian curves of the XRD peaks from $2\theta = 43°$ to $2\theta = 45.7°$. (A) $F_T$ (002), (020), $F_R$ (202), (B) $F_R$ (202).

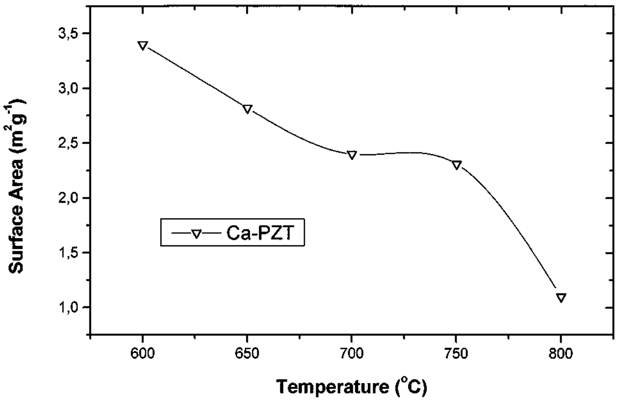

*Figure 7* Surface area of ZT/PbO-CaO and Ca-PZT phases from 600° C to 800°/3 h.

between particles occurs. The observed reduction of surface area of the ZT crystalline phase, (Fig. 2) caused by the oxalate precipitation, happened at 600°C between 70.00 $m^2/g$ to 3.25 $m^2/g$.

Comparisons between the particle size obtained by BET and the Scherrer equation by using XRD, (Fig. 8) shows an increase of crystal size and strong decreases of average particle size. Reduction of surface area shows the same tendency of decrease in the average particle size. At the beginning of resin decomposition an amorphous formation is formed at the presence of decomposed salt and due to this, strong agglomerate was formed. During the crystallization of Ca-PZT kinetic temperature led to decomposition of agglomerates, observed by a decrease of average particle size. Due to a break-up of agglomerate particles an increase of grain distributions occurs and diminished the average particle size, however an increase of single particle, due to

TABLE II Surface areas of ZT phase and Ca-PZT phase and average particle size of Ca-PZT

| Temperature (°C) | S.A.(ZT) ($m^2/g$) | S.A.(Ca-PZT) ($m^2/g$) | A.P.S.(Ca-PZT) (nm) |
|---|---|---|---|
| 350 | 110 | – | – |
| 550 | 105 | – | – |
| 600 | 69 | 3.25 | 250 |
| 700 | 22 | 2.40 | 350 |
| 800 | – | 1.20 | 370 |

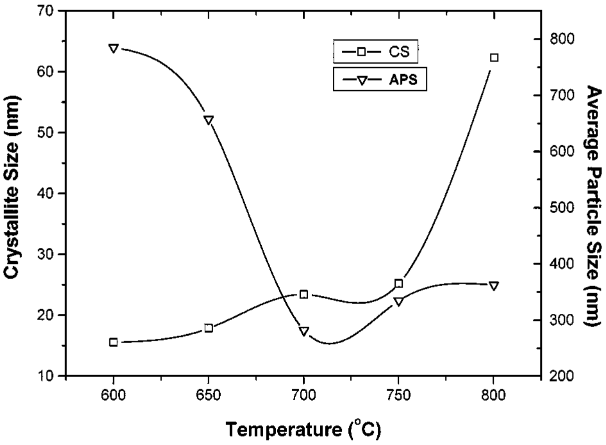

*Figure 8* Comparisons between crystallite size (nm) and average particle size (nm) of Ca- PZT from 600° C to 800° C/3 h.

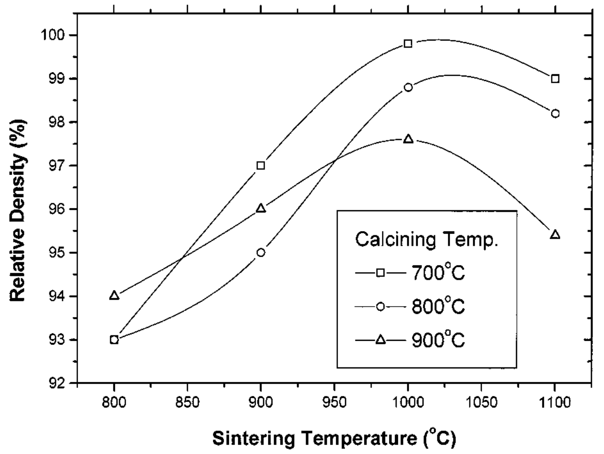

*Figure 9* Relative density of sintered powder between 800° C until 1100° C for different calcination temperatures.

the kinetic effect of the diffusion process, was observed by using the Scherrer equation.

Table II shows a strong decrease of surface area during the reactions between the ZT and Ca-PZT formation. According XRD analysis the Ca-PZT phase is totally formed at 700°C. Close to 700° C the surface area of 2.4 $m^2/g$ and average particle size of 350 nm demonstrated that high sinterability could be obtained.

Analysis of sintered powder, (Fig. 9) shows that the apparent density of the calcined powder decreased on increasing sintering temperature. An optimization was observed at 700°C/2 h with values of $\rho/\rho o = 99.9\%$. Kinetic effect of powder morphology due to a process control led to single phase ZT and Ca-PZT at low temperature with high homogeneity and sinterability, which led to dense Ca-PZT synthesis. Studies of calcium doped PZT by using coprecipitation method [26] shows approximately 98.4% of apparent density. Inferior measures of electrical characteristics of Ca-PZT are attributed to the small values of density obtained with the additions of calcium. The low sinterability of calcium is attributed to the low diffusion of $Ca^{+2}$ caused by large ionic radii. During the competition between the ions in the lattice there is a high activation energy necessary for ion diffusion. Chemical processing leads to an approximation at atomic level and diminishes the path of diffusion in the lattice.

## 4. Conclusions

The ZT phase synthesis processed by polymeric precursors leads to high homogeneous powder formations, narrow average particle size, surface area from 108 $m^2/g$ at 550° C to 22 $m^2/g$ at 700° C/3 h with high crystallinity.

Decomposition of ZT/$PbC_2O_4$ – $CaC_2O_4$ shows a formation of a PbO phase under the ZT phase, and the formation of $F_T$ and $F_R$ at 550°C which was transformed to $F_T$ phase in Ca-PZT at nearly to 700°C/3 h. Sintering with different calcining temperatures shows that optimum powder characteristics were observed at 700°C/3 h reaching 98.8% of relative density at 1000° C/3 h. Such processing leads to high homogeneity of phases and inhibits a loss of mass occuring during the sintering of PZT which diminishes the bulk density.

## References

1. B. JAFFE, W. R. COOK and H. JAFFE, "Piezoeletric Ceramics" (ACADEMIC PRESS, LONDON, 1971).
2. H. KANAI, FURUKAWA, H. ABE and O. YAMASHITA, *J. Amer. Ceram. Soc.* **77** (1994) 2620.
3. M. TAKAHASHI, *Jpn. J. Appl. Phys.* **5** (1971) 643.
4. T. YAMAMOTO, *Amer. Ceram. Soc. Bull.* **71** (1992) 978.
5. J. F. LOSANO and C. MOURE, *Bol. Soc. Esp. Vidr.* **71** (1992) 978.
6. K. KAKEGAWA, J. MOHRI, T. TAKAHASHI, H. YAMAMURA and S. SHIRASAKI, *J. Amer. Ceram. Soc.* **68** (1985) C 205.
7. K. KAKEGAWA, K. ARAI, Y. SASAKI and T. TOMIZAWA, *ibid.* **71** (1988) C 49.
8. V. A. ISOPOV, *Sov. Phys. Solid State* **18**(4) (1976) 529.
9. S. A. MABUD, *J. Apl. Cryst.* **13** (1980) 211.
10. S. S. CHANDRATREYA, R. M. FULRATH and J. A. PASK, *J. Amer. Ceram. Soc.* **64** (1981) 422.
11. G. TOMANDL, A. STIEGELSCHMIT and R. BOHNER, "Science Of Ceramics Chemical Processing, Part I: Sol-Gel Science" (John Wiley & Sons, New York, 1986).
12. M. CERQUEIRA, R. S. NASAR, E. LONGO, E. R. LEITE and J. A. VARELA, *Mat. Lett.* **22** (1995) 181.
13. J. C. FERNANDEZ, D. A. HALL and G. N. GREAVES, in "European Powder Diffraction: EPPIC IV, Part 1 and 2," 1996, p. 228, pp. 411–416.
14. B. G. MURALIDHARAN, A. SENGUPTA, G. S. RAO and D. C. AGRANAL, *J. Mater. Sci.* **30** (1995) 3231.
15. M. A. ZAGHETE, J. A. VARELA, E. LONGO and Y. P. MASCARENHAS, *J. Amer Ceram. Soc.* **75** (1992) 2089.
16. S. KIM, G. S. LEE, T. R. SHROUT and S. VENKATARAMANI, *J. Mater. Sci.* **26** (1991) 4411.
17. T. KIMURA, A. TAKENAKA, T. MIFUNE, Y. HAYASHI and T. YAMAGUCHI, *ibid.* **27** (1992) 1476.
18. J. H. CHOY, Y. S. HAN and J. T. KIM, *J. Mat. Chem.* **5** (1995) 65.

19. R. K. M. RAO, A. V. P. RAO and S. KOMARNEMI, *Mat. Lett* **28** (1996) 463.
20. M. CERQUEIRA, R. S. NASAR, E. R. LEITE, E. LONGO and J. A. VARELA, *ibid.* **35** (1998) 166.
21. R. S. NASAR, M. CERQUEIRA, E. LONGO, E. R. LEITE, J. A. VARELA, A. BELTRAN and J. ANDRES, *J. Mater. Sci.* **34** (1999) 3659.
22. M. CERQUEIRA, Master Degree, Federal University of São Carlos, São Carlos, Brazil, 1992.
23. R. J. HILL and B. E. REICHERT, *J. Amer. Ceram. Soc.* **73** (1990) 2822.
24. J. A. NAVIO, F. J. MARCHENA, M. MACIAS, P. J. SANCHEZ-SOTO and P. PICHAT, *J. Mater. Sci.* **27** (1992) 2463.
25. E. R. LEITE, M. CERQUEIRA, M. PERAZOLI, R. S. NASAR, E. LONGO and J. A. VARELA, *J. Amer. Ceram. Soc.* **79** (1996) 1563.
26. M. CERQUEIRA, R. S. NASAR, E. LONGO, J. A. VARELA, A. BELTRAN and J. ANDRES, *J. Mater. Sci.* **32** (1997) 2381.

*Received 7 October 1999*
*and accepted 6 July 2000*